Analytical and Experimental Investigation of Melting Heat Transfer

C. Wen,* J. W. Sheffield,† and M. P. O'Dell*
University of Missouri–Rolla, Rolla, Missouri
and
J. E. Leland‡
Air Force Wright Aeronautical Laboratories, Wright-Patterson Air Force Base, Ohio

A computational model is presented for the prediction of the heat transfer between a heat-transfer fluid (HTF) and a phase change material (PCM) of a latent heat storage unit. Two models of flow, hydrodynamically fully developed and developing, of the HTF were proposed in this study. A two-dimensional enthalpy method was used for the computation of the phase change heat transfer in the PCM. A fully implicit finite-difference scheme was utilized for the calculation of convective heat transfer in the HTF. The unknown time-dependent boundary condition between the HTF and the PCM was found iteratively. The predictions were substantiated by their fair agreement with experimental data. Factors affecting the heat-transfer rates between the HTF and the PCM were studied numerically for both the hydrodynamically fully developed and developing flows. It was found that the Nusselt number is significantly increased by the developing temperature profiles. The developing velocity profiles also increased the Nusselt number. However, the influence on Nusselt number due to the developing velocity profiles was less significant than that due to the developing temperature profiles. Other factors affecting the Nusselt number are discussed.

Nomenclature

A = area
A_1, A_2, A_3 = constant
B = constant
c = specific heat
C = constant
D' = diameter
D'_h = hydraulic diameter, $2(r'_0 - r'_2)$
Fo = Fourier number, dimensionless time, Eq. (7)
h = heat-transfer coefficient
i = specific enthalpy
k = thermal conductivity
L = length of tube, $L'/RePrD'_0$
L' = length of tube
M = constant
Nu = Nusselt number
p = pressure, $p'/(\rho u'^2_m/2)$
p' = pressure
Pr = Prandtl number, ν/α
q = heat flow rate
Q = heat flow per length
Q_{x1}, Q_{x2} = local heat flow per length
r = spatial coordinate, r'/r'_0
r' = spatial coordinate
Re = Reynolds number, $u'_m D'_h/\nu$
Re' = Reynolds number, $2u'_m r'_0/\nu$
Ste = Stefan number, Eq. (39)
t = time
T = temperature, $(T' - T'_f)/(T'_e - T'_f)$
T' = temperature
u' = axial component of velocity
U = specific internal energy
v' = radial component of velocity
V = control volume
x = spatial coordinate, $x'/Re'r'_0$
x' = spatial coordinate
X = spatial coordinate, $x'/RePrD'_h$
Z = spatial coordinate, x'/Rer'_0
α = thermal diffusivity
Δ = step size
ε = convergence criteria
θ = enthalpy, Eq. (5)
$\tilde{\theta}$ = scaled dimensionless enthalpy, Eq. (28)
λ = latent heat of fusion
ν = kinematic viscosity
ρ = density
τ = dimensionless time, $\alpha_h t/r'^2_0$
ϕ = scaled dimensionless temperature, Eq. (8)
χ = spatial coordinate, x'/r'_1

Superscripts

m = time level
$*$ = saturated state

Subscripts

b = mean bulk value
e = at the inlet
f = fusion
h = heat-transfer fluid
i = spatial location
ini = initial value
j = spatial location
l = liquid region
m = mean value
max = maximum value
p = phase change material
t = tube
0 = at the shell wall
1 = at the inner-wall of tube
2 = at the outer wall of tube

Presented as Paper 88-0357 at the AIAA 26th Aerospace Sciences Meeting, Reno, NV, Jan. 11–14, 1988; received Jan. 25, 1988; revision received May 27, 1988.

*Research Assistant.
†Associate Professor of Mechanical and Aerospace Engineering.
‡Mechanical Engineer.

Introduction

THE high-power requirements of future spacecraft missions present many technological challenges to the designers of spacecraft thermal management systems (SCTMS). The need to buffer thermal loads, such as during burst power conditions, is currently a major problem. One possible solution is the application of latent heat storage with its use of phase change materials (PCM) to buffer the large heat input conditions. The present investigation was motivated by the need for predictive tools necessary for the design of SCTMS using latent thermal energy storage. In this research, a latent heat storage unit is configured as shown in Fig. 1. The PCM is contained in a long horizontal tube assembled within a cylindrical shell. The temperature-controlled heat-transfer fluid (HTF) is pumped through the shell-and-tube heat exchanger to release or absorb thermal energy to or from the PCM.

Basically, the analysis of heat transfer in this latent heat storage unit is divided into two problems: the melting/freezing problem of the PCM in a horizontal tube and the convective heat-transfer problem of the HTF in an annular passage.

For the present melting/freezing problem, the unknown tube wall temperature is assumed to be time and location dependent. This problem is rather difficult to solve because of the moving boundary and the unknown wall temperature. By introducing the enthalpy method, this problem becomes much simpler. The governing equation of the enthalpy method is similar to the single-phase conduction equation. Using the enthalpy method to approach a phase change problem has the following advantages: 1) there are no conditions to be satisfied at the phase change boundary; 2) there is no need to accurately track the phase change boundary; 3) there is no need to consider the solid and liquid sides separately; and 4) it allows a mushy zone between the solid and liquid phases. The unknown tube wall temperature between the heat-transfer fluid and the PCM is obtained from an energy balance. However, an iterative procedure is required. The Newton-Raphson method is used for this "root-finding" problem.

One of the objectives of this research is to develop a numerical method to find the heat transfer between the HTF and the PCM. The comprehensive understanding of the heat transfer in the latent heat storage system can provide the information for the design of microgravity spacecraft thermal management systems. However, there are many other applications, such as metal casting, crystal growth, and thermal energy storage for building space conditioning, where the fundamental understanding of the phase change phenomena is important.

Literature Review

Melting/Freezing Heat Transfer in Horizontal Cylinders

The heat-transfer processes that occur during melting/freezing in horizontal cylinders have recently received considerable attention because of a wide range of engineering applications. Mathematically, the problem belongs to the "moving boundary" class of problem. Webb and co-workers[1] studied the melting phenomenology of water in a horizontal cylindrical capsule by experiment. The solid/liquid interface and the interaction of fluid flow, caused by natural convection and the motion of the solid induced by the density inversion of the water/ice system, were determined visually. Heat transfer at the solid/liquid interface during melting from a horizontal cylindrical heat source embedded in a PCM was studied by Bathelt and Viskanta.[2] Two paraffins, n-heptadecane, $T'_f = 22.2°C$ and n-octadecane, $T'_f = 28.2°C$ were used as the PCM's. The shape of the solid/liquid interface was determined photographically and the local heat-transfer coefficients were measured using a shadowgraph technique. Ho and Viskanta[3] and Pannu et al.[4] used the vorticity-stream function method to deal with the problem of phase change in horizontal cylinders. This method is based on the consideration that the heat transfer in the liquid PCM is by natural convection. A perturbation method was used by Yao and Chen[5] to solve the melting problem in a horizontal cylinder. This method is complex, tedious, and limited to small Stefan numbers. Rieger et al.[6,7] used a numerically generated coordinate system, which conformed to the shape of the boundaries, to study the melting process around a horizontal cylinder. Because of the changing shape of the solid/liquid interface, this method appears to be laborious.

All the aforementioned studies did not consider the temperature variation of the PCM in the axial direction. Also, most were limited to uniform tube wall temperature. Experimental studies also focused on uniform tube wall temperature cases. McCabe[8] obtained numerical solutions for time-dependent temperature distributions. He used the enthalpy method with an implicit scheme to solve the melting/freezing problem in cylinders. However, only radial solutions were obtained. Like the other researchers, he also did not take the axial dependence into account. In terms of the conjugate heat-transfer problems involving the HTF and the PCM with "natural" boundary conditions at the interface, several papers[9–11] have addressed the problem of freezing on the outside of a horizontal cylinder.

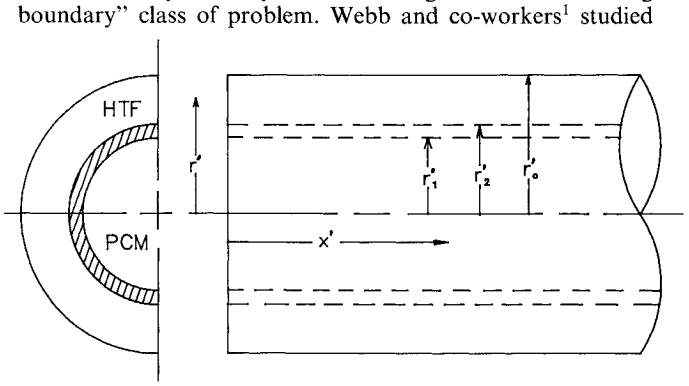

Fig. 1 Latent heat storage unit and coordinate system.

Heat Transfer in Annular Passages

The annulus represents a common geometry employed in a variety of heat-transfer systems ranging from simple heat exchangers to the most complicated nuclear reactors. Theoretical and numerical studies of heat transfer in an annulus can be roughly divided into two types: heat transfer in a hydrodynamically fully developed region and heat transfer in an entry region.

Heat Transfer in Hydrodynamically Fully Developed Region

For the case of an axially symmetric hydrodynamically fully developed fluid flow with constant properties in a concentric annulus, Reynolds et al.[12] concluded that there are four types of fundamental boundary conditions of interest: 1) a step temperature on one wall and the other wall maintained at the inlet temperature, 2) uniform heat flux at one wall and the other wall being kept adiabatic, 3) uniform wall temperature at one wall and the other wall remaining insulated, and 4) uniform heat flux from one wall with the opposite wall maintained at the inlet temperature. A very thorough treatment of the annulus problem has been published by Lundberg et al.[13] based on these four types of fundamental solutions. They used an eigenvalue method to yield an exact solution for the entire thermal entrance region, but near the point of a step change in either the wall temperature or the heat flux at the wall, a large number of terms in the eigenfunction expansion are required. Worsoe-Schmidt[14] obtained these four types of fundamental solutions by using a similarity transformation method. The similarity variable used was obtained from Leveque solution. Hatton and Quarmby[15] also used the eigenvalue method to find solutions of heat transfer in annuli. However, only the cases with either uniform wall temperature

or uniform heat flux on the inside wall and with the outside wall insulated were analyzed. The case of an arbitrarily prescribed heat flux around the periphery of either wall, or both walls, was studied by Sutherland and Kays.[16] The technique used was an expansion of the known peripheral heat flux distribution in a Fourier series. Because the resulting temperature distribution can also be expressed as a Fourier series, the energy equation becomes a set of ordinary differential equations in terms of the eigenfunction. These eigenfunctions were used with the Fourier coefficients of any peripheral heat flux distribution to obtain the resulting wall temperature distribution.

Heat Transfer in Entry Region

The solution of the heat-transfer problem with simultaneous development of velocity and temperature fields has been the subject of a great deal of attention during the past three decades. Because the temperature profile cannot be obtained without knowing the velocity profile, the solution is usually obtained by first solving the hydrodynamic entry length problem and then solving the thermal entry length problem.

Murakawa[17] has obtained an approximate entrance length solution for the annulus via a series solution. The final result only partially satisfies the boundary conditions. Liron and Gillis[18] also obtained solutions for flow in an annular region by representing the momentum equation by the stream function and then by using an eigenvalue method. However, the solution is restricted to vanishingly small Reynolds numbers. Heaton et al.[19] obtained a velocity profile defined over the entire region by linearizing the momentum equation and solving the resulting equations analytically.

For the thermal entry length problem, Murakawa[17] has obtained a solution for an arbitrary wall temperature at the inner wall of the annulus by an integral method. The developing velocity and temperature profiles used were simplified and were applicable only near the inner wall. The resulting solution did not show all the geometric effects nor did it approach the fully developed solution. Heaton et al.[19] linearized the energy equation to find the temperature profile. Their solution was obtained by an integral method. However, the only solution obtained was the case of uniform heat flux at one wall and the other wall insulated.

Analysis

Enthalpy Model for Phase Change

For an arbitrary control volume V that is fixed in space and if conduction is the only heat-transfer mechanism to be considered, the time rate of change of internal energy has to be equal to the net rate at which heat is conducted through V if there is no energy source inside V and no external work toward V. Mathematically, this can be expressed by

$$\frac{\mathrm{d}}{\mathrm{d}t}\int_V \rho U \,\mathrm{d}V = \int_A k\nabla T\cdot\hat{n}\,\mathrm{d}A \tag{1}$$

It is noted that in the absence of motion, the pressure P is independent of time. Thus,

$$\frac{\mathrm{d}}{\mathrm{d}t}\int_V P\,\mathrm{d}V = 0 \tag{2}$$

Since

$$\rho U = \rho i - P \tag{3}$$

Equation (1) can be written in the form

$$\frac{\mathrm{d}}{\mathrm{d}t}\int_V \rho i\,\mathrm{d}V = \int_A k\nabla T\cdot\hat{n}\,\mathrm{d}A \tag{4}$$

Equation (4) is the general form of enthalpy equation. The i vs T relationship for the phase change material is used in conjunction with Eq. (4). Frequently, the dimensionless enthalpy θ is defined as

$$\theta = \frac{1}{\rho V}\int_0^V \frac{\rho(i-i_l^*)}{\lambda}\,\mathrm{d}V \tag{5}$$

For the case of melting/freezing process in a horizontal tube, θ for the control volume as shown in Fig. 2 is

$$\theta = \frac{2}{\rho(r_{i+1}'^2 - r_i'^2)\Delta x'}\int_0^V \rho\frac{(i-i_l^*)}{\lambda}\,\mathrm{d}V \tag{6}$$

if the bouyancy effect in the liquid PCM is neglected and the density is assumed to be constant.

Introducing θ, Fo, and ϕ, such that

$$Fo = \alpha t/r_1'^2 \tag{7}$$

and

$$\phi = C_p(T' - T_l'^*)/\lambda \tag{8}$$

into Eq. (4), one has

$$\left.\frac{\partial\theta}{\partial Fo}\right|_{i,j} = \left(\left.\frac{\partial\phi}{\partial\chi}\right|_{i,j+1} - \left.\frac{\partial\phi}{\partial\chi}\right|_{i,j}\right)\frac{1}{\Delta\chi} + \frac{2}{r_{i+1}^2 - r_i^2} \times\left(\left.\frac{\partial\phi}{\partial r}\right|_{i+1,j}\cdot r_{i+1} - \left.\frac{\partial\phi}{\partial r}\right|_{i,j}\cdot r_i\right) \tag{9}$$

Forward difference in time and backward difference in space, the explicit finite-difference representation of Eq. (9) is

$$\frac{\theta_{i,j}^{m+1} - \theta_{i,j}^m}{\Delta Fo} = \frac{\phi_{i,j+1}^m + \phi_{i,j-1}^m - 2\phi_{i,j}^m}{\Delta\chi^2} + \frac{2}{r_{i+1}+r_i} \frac{[(\phi_{i+1,j}^m - \phi_{i,j}^m)r_{i+1} - (\phi_{i,j}^m - \phi_{i-1,j}^m)r_i]}{\Delta r^2} \tag{10}$$

The relationships between θ and ϕ are

$$\phi = \theta \quad \text{when} \quad \theta \geq 0 \tag{11a}$$

$$\phi = 0 \quad \text{when} \quad -1 \leq \theta \leq 0 \tag{11b}$$

$$\phi = \theta + 1 \quad \text{when} \quad \theta < -1 \tag{11c}$$

Equation (10) should be used in conjunction with the energy equation and the momentum equation for the HTF, since the conditions between the HTF and PCM are functions of time and location. Because of the unknown boundary condition between the PCM and HTF, the implicit scheme of the finite-difference equation for the enthalpy model seems impossible. The explicit scheme is therefore used since it is the more straightforward method.

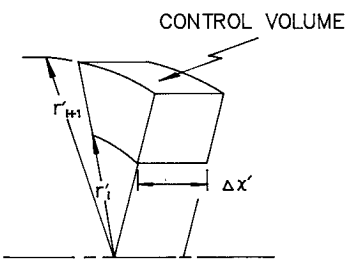

Fig. 2 Control volume in cylindrical coordinates.

Heat Transfer in an Annular Passage

The current problem of interest is heat transfer in an annular passage with a transient temperature distribution. The dimensionless differential equations associated with this problem are the continuity, momentum, and energy equations

$$\frac{\partial u}{\partial x}+\frac{1}{r}\frac{\partial (rv)}{\partial r}=0 \tag{12}$$

$$u\frac{\partial u}{\partial x}+v\frac{\partial u}{\partial r}=-\frac{1}{2}\frac{\mathrm{d}p}{\mathrm{d}x}+2\left(\frac{\partial^2 u}{\partial r^2}+\frac{1}{r}\frac{\partial u}{\partial r}\right) \tag{13}$$

$$\frac{\partial T}{\partial \tau}+\frac{Pr}{2}\left(u\frac{\partial T}{\partial x}+v\frac{\partial T}{\partial r}\right)=\frac{\partial^2 T}{\partial r^2}+\frac{1}{r}\frac{\partial T}{\partial r} \tag{14}$$

These equations assume steady, laminar, incompressible flow with constant fluid properties and negligible axial conduction, buoyancy effect, internal energy generation, viscous energy dissipation, and axial rate of change of the radial shear stress. However, for the current problem, the flowing fluid temperature is time dependent. Therefore, the energy equation is transient. The boundary conditions for these equations are given by

$$u(x,r_2)=v(x,r_2)=0 \tag{15}$$

$$u(x,1)=v(x,1)=0 \tag{16}$$

$$u(0,r)=u_e(r) \tag{17}$$

$$T(\tau,x,r_2)=T_2(\tau,x) \tag{18}$$

$$\frac{\partial T(\tau,x,1)}{\partial r}=0 \tag{19}$$

$$T(\tau,0,r)=T_e(t) \tag{20}$$

Equation (19) indicates that the shell is insulated at $r=1$. In addition to these geometric boundary conditions, an initial boundary condition is required for Eq. (14).

Hydrodynamically Fully Developed Flow

If the flow is hydrodynamically fully developed, then the velocity is independent of x and Eq. (13) becomes

$$\frac{\partial^2 u}{\partial r^2}+\frac{1}{r}\frac{\partial u}{\partial r}=\frac{1}{4}\frac{\mathrm{d}p}{\mathrm{d}x}=\text{const} \tag{21}$$

The integration of Eq. (21) with the boundary conditions defined by Eqs. (15) and (16) leads to Lamb's[20] fully developed velocity profile for the annulus,

$$u=(2/M)\,(1-r^2+B\ell n\, r) \tag{22}$$

where

$$B=(r_2^2-1)/\ell n\, r_2 \quad \text{and} \quad M=1+r_2^2-B$$

Flow in the Entrance Region

The problem of laminar flow heat transfer in the entrance region was extensively studied during the past three decades. However, many of these studies were limited to some simple cases such as uniform heat flux, uniform wall temperature, and steady-state temperature distribution. For the current problem of a transient temperature distribution, none of the previous studies can be applied directly and therefore a re-examination is necessary.

In order to find the velocity distribution, an additional equation is required since there are three unknowns, u, v, and p, appearing in Eqs. (12) and (13). The integral continuity equation is used,

$$\int_{r_2}^{1} ru\,\mathrm{d}r=\frac{1-r_2^2}{2} \tag{23}$$

Because momentum equation [Eq. (13)], is nonlinear in u, it is difficult to solve by analytical methods. Instead, a direct numerical method is used to solve this problem.

To find the temperature distributions in the flowing fluid and the heat fluxes between the flowing fluid and the PCM, the energy equation must be solved. If the velocities and the boundary conditions for the energy equation are known, it is not difficult to solve the problem; however, if the boundary condition between the flowing fluid and the PCM is unknown, a technique of finding the boundary condition is needed.

Numerical Procedure

Velocity Profiles in the Entrance Region

Although some methods[17–19] were used previously to find the laminar velocity distribution of an annular passage in the entrance region, the previous methods are complicated and therefore are not very practical for this study. A much simpler method will be used.

By choosing an arbitrary value for p_j, there are then only two unknowns, u and v. The procedure of finding u and v is: 1) give an arbitrary value for v; 2) solve u by the Gaussian elimination method; 3) solve v by the Gaussian elimination method; 4) compare the new u with that in the previous iteration. If the difference is sufficiently small, the u and v obtained can be considered satisfied for the value of p_{j-1}; otherwise, using the new value of u and v and return to step 2. Since u and v are obtained by choosing an arbitrary value for p_j, u may or may not satisfy the integral continuity equation. An iterative solution for p_j is required and the value of p_j is considered to be converged if and only if

$$\left|\int_{r_2}^{1} ru\,\mathrm{d}r-\frac{1-r_2^2}{2}\right|\le\varepsilon \tag{24}$$

where ε is the convergence criteria. The strategy to find p_j is that if the chosen value of p_j is smaller than the exact value, then

$$\int_{r_2}^{1} ru\,\mathrm{d}r<\frac{1-r_2^2}{2}$$

and a larger value of p_j is used in next iteration. The Newton-Raphson method is used to find p_j.

Iterative Solution of the Inner-Wall Tube Temperature

Since the enthalpy equation nor the energy equation can be used without giving the temperature distribution between the heat-transfer fluid and the PCM, the iterative solution of the inner tube wall temperature T_1' becomes a starting procedure for the calculation of the heat transfer in the latent thermal storage system. Since this temperature is between the inlet fluid temperature and the initial PCM temperature, the iterative solution converges.

Solving the Melting/Freezing Problem

The boundary conditions of Eq. (9) are given by

$$\phi|_{r=r_1}=\frac{\rho C_p(T_1'-T_f')}{\lambda} \tag{25}$$

$$\left.\frac{\partial \phi}{\partial r}\right|_{r=0}=0 \tag{26}$$

$$\left.\frac{\partial\phi}{\partial\chi}\right|_{\chi=0} = \left.\frac{\partial\phi}{\partial\chi}\right|_{\chi=L} = 0 \tag{27}$$

Equation (27) is based on the assumption that the two end plates for the PCM tube have very low thermal conductivities so that they are considered to be adiabatic.

The enthalpy distribution in the PCM at a fixed axial location can be easily obtained by using Eq. (10) and the appropriate boundary conditions. The temperature distribution is obtained from Eq. (11). The new θ from the last time step is a result of radial and axial conductions during the time step. The θ obtained from Eq. (10) is not appropriate to be used for the calculation of the heat flux between the heat-transfer fluid and the PCM. The equation that resembles Eq. (10) but lacks the axial conduction term is given below and is used for the purpose of calculating the heat flow,

$$\frac{\tilde{\theta}_{i,j}^{m+1} - \theta_{i,j}^{m}}{\Delta\tau} = \frac{2}{r_{i+1}+r_i}\frac{[(\phi_{i+1,j}^{m} - \phi_{i,j}^{m})r_{i+1} - (\phi_{i,j}^{m} - \phi_{i-1,j}^{m})r_i]}{\Delta r^2} \tag{28}$$

where

$$\tilde{\theta} = \frac{2}{\rho(r_{i+1}'^2 - r_i'^2)\Delta x'}\int_0^V \rho\frac{(i-i_f^*)}{\lambda}\,dV$$

The transient local heat flow rate for a length of $\Delta x'$ at $r = r_1$ is given by

$$q(t,x') = \frac{\sum V_i\rho_p\lambda(\tilde{\theta}_i^{m+1} - \theta_i^m)}{\Delta t'} \tag{29}$$

where

$$V_i = \pi(r_{i+1}'^2 - r_i'^2)r_1^2\,\Delta x' \quad \text{and} \quad \Delta t' = \Delta\tau r_1'^2/\alpha_p$$

Therefore, the transient local heat flow per unit length is given by

$$Q_{x1}(t,x') = (q(t,x')/\Delta x') \tag{30}$$

Transient Temperature Distribution of the Heat Transfer Fluid

From the integration of the one-dimensional heat conduction equation for cylindrical coordinates with the boundary conditions such that

$$T' = T_1' \quad \text{at} \quad r' = r_1'$$
$$T' = T_2' \quad \text{at} \quad r' = r_2'$$

and using Fourier's law, one has

$$Q = \frac{2\pi k_t(T_2' - T_1')}{\ell n(r_2'/r_1')} \tag{31}$$

where Q is the heat flow rate through the PCM tube per unit length.

Equation (31) is obtained based on the assumptions that the tube wall is very thin so that the axial conduction and the sensible heat absorbed by the tube are neglected. Since the heat flow through the PCM tube is equal to the heat flow from the PCM tube to the PCM, from Eqs. (30) and (31) one has

$$T_2'(t,x') = \frac{Q_{x1}(t,x')\cdot\ell n(r_2'/r_1')}{2\pi k_t} + T_1'(t,x') \tag{32}$$

Upon finding the temperature distribution of the HTF, the Nusselt numbers can then be calculated. According to Fourier's law, the local heat flow per unit length between the heat transfer fluid and the PCM can be given by

$$Q_{x2}(t,x') = 2\pi r_2' k_h \left.\frac{\partial T'}{\partial r'}\right|_{r'=r_2'} \tag{33}$$

The bulk temperature of the heat-transfer fluid is

$$T_b = \int_{r_2}^{1} uTr\,dr \Big/ \int_{r_2}^{1} ur\,dr \tag{34}$$

By definition, the Nusselt number is

$$Nu = \frac{hD_h}{k_h} = \frac{2h(r_0' - r_2')}{k_h} \tag{35}$$

The heat flux by conduction at the outer PCM tube surface is equal to the heat flux by convection to the HTF. Thus,

$$h(T_b' - T_2') = k_h \left.\frac{\partial T'}{\partial r'}\right|_{r'=r_2'} \tag{36}$$

The combination of Eqs. (35) and (36) yields

$$Nu = \frac{2(1-r_2)}{T_b - T_2}\left.\frac{\partial T}{\partial r}\right|_{r=r_2} \tag{37}$$

It is remembered that all the values concerning the heat transfer between the heat-transfer fluid and the PCM and the values concerning the melting/freezing in the PCM are based on the iterative T_1' and it may not be converged. T_1' is considered to be converged if and only if

$$|Q_{x1} - Q_{x2}| \le \varepsilon \tag{38}$$

where ε is the convergence criteria. If T_1' is not converged, then one has to correct it and return to the solution procedure of solving the melting/freezing problem. This is a root finding problem and T_1' is found by the Newton-Raphson method.

Experiment

This experimental study focused on the melting process of a contained PCM. The results are compared with the numerical results. P116, a Sun wax with a melting point temperature of 43°C was chosen as the PCM since it is transparent in the liquid state but opaque in the solid state, thus providing visual identification of the melting interface.

The experimental apparatus employed in this study is shown schematically in Fig. 3. The experimental setup consists of three major systems: instrumented heat exchanger, fluid flow control, and data acquisition. Details of the experimental apparatus are given in Ref. 21.

An experimental investigation of the melting process was conducted. Thermal equilibrium was established in the heat storage unit at a temperature of 39°C. Fluid flow was shut off to the heat exchanger. Once the bath temperature reached 49°C, fluid flow was initiated into the heat exchanger and the data acquisition process was begun. When the experiment was in progress, the flow rate was constant at 0.65 gal/min (2.46 liter/min) and the inlet temperature of the HTF was also constant at 49°C. The melting process of the PCM was recorded by the VCR for later study.

Verification of Accuracy

Since in recent studies many of the methods used are either new or improved from other methods, a comparison of the recent numerical results with experimental results or the results obtained by others is very important. This not only avoids mistakes made in recent studies, but also provides an examination of the accuracy of recent methods.

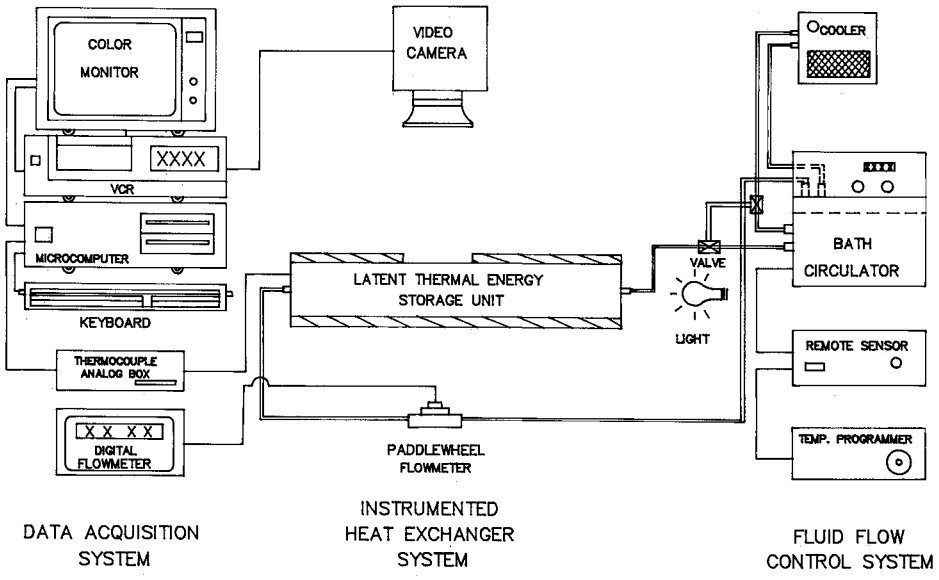

Fig. 3 Experimental apparatus.

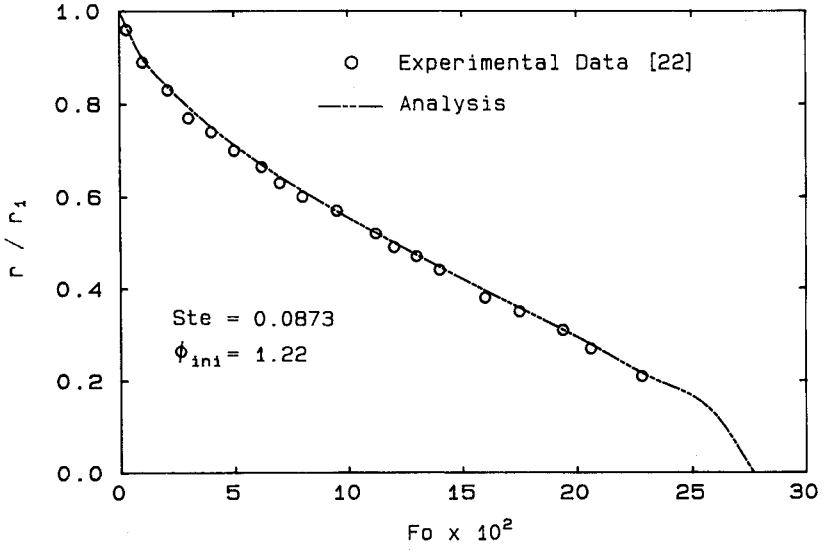

Fig. 4 Comparison of predicted solid-liquid interface positions with data for solidification of n-heptadecane.

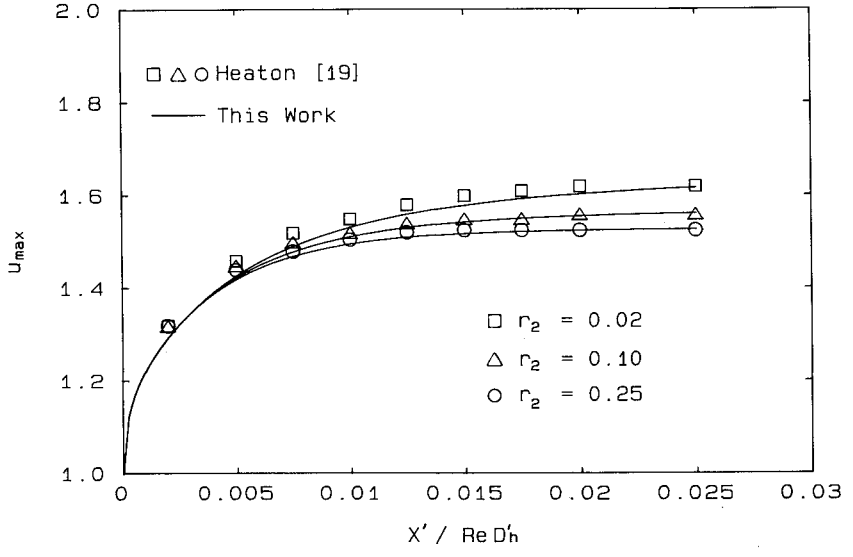

Fig. 5 Maximum velocity variation in the entrance region of an annulus.

Table 1 Velocity distributions in fully developed region for $r_2 = 0.5$

$\frac{r - r_2}{1 - r_2}$	Numerical method		
	11 grids	41 grids	Eq. (22)
0.1	0.60266	0.60278	0.60279
0.2	1.03899	1.03912	1.03913
0.3	1.32605	1.32616	1.32616
0.4	1.47716	1.47721	1.47721
0.5	1.50284	1.50283	1.50283
0.6	1.41159	1.41154	1.41153
0.7	1.21036	1.21029	1.21028
0.8	0.90493	0.90485	0.90485
0.9	0.50011	0.50006	0.50006

Table 2 Solutions of flow in fully developed region for $r_2 = 0.5$

X	Nu		
	Present	Lundberg	Worsoe-Schmidt
	Constant heat flux at inner wall		
0.0001	34.985	34.6	34.233
0.0010	16.39	16.4	16.356
0.0025	12.378	12.37	12.367
0.005	10.132	10.13	10.127
0.010	8.435	8.433	—
0.025	6.932	6.931	—
0.05	6.353	6.353	—
0.1	6.191	6.192	—
	Constant temperature at inner wall		
0.0001	29.802	28.4	28.456
0.0010	13.760	13.68	13.701
0.0025	10.445	10.42	10.427
0.005	8.610	8.602	8.603
0.010	7.249	7.246	7.247
0.025	6.118	6.117	—
0.05	5.784	5.785	—
0.1	5.738	5.738	—

It is found that many of the previous studies were restricted to limited boundary conditions or simpler cases; therefore, the comparisons with previous works are quite limited.

Melting/Freezing of PCM in a Horizontal Tube

A comparison of the experimental data of Viskanta and Gau[22] and the predictions by the enthalpy method with n-heptadecane as the PCM, given in Fig. 4, shows quite good agreement. In Fig. 4 the Stefan number Ste and the initial dimensionless temperature ϕ_{ini} are defined as

$$Ste = \frac{c_p(T'_f - T'_1)}{\lambda} \tag{39}$$

$$\phi_{\text{ini}} = \frac{T' - T'_1}{T'_f - T'_1} \tag{40}$$

Entrance Region Velocity Distribution

The method used in this investigation to find the laminar velocity distribution in the entrance region of an annulus is very simple when compared with the eigenvalue method. When computing on an IBM 4381 system for 41 × 501 grids, the CPU time is only 86 s. The comparison of maximum velocity distribution by Heaton et al.[19] and this work is given in Fig. 5. When the flow is fully developed, the velocity profile obtained by this method has a maximum difference of only 0.02% compared with Eq. (22) for the case of $r_2 = 0.5$ and 11 grid points in the radial direction. A comparison of the fully developed velocity profiles obtained from Eq. (22) and from the numerical method for $r_2 = 0.5$ are shown in Table 1.

Table 3 Solutions of uniform heat flux at inner wall for flow in entry region with $Pr = 10$

X	Nu		
	Present	Neglect v	Heaton
0.0010	16.081	16.468	16.68
0.0025	12.255	12.535	12.60
0.005	10.079	10.187	10.20
0.01	8.414	8.453	8.43

Heat Transfer in Annular Passages

Comparisons of the results for heat transfer in annular passages for flow in the fully developed region with Lundberg et al.[13] and Worsoe-Schmidt's[14] are given in Table 2. For flow in the entrance region, the results compared with Heaton's[19] for the case of uniform heat flux at the inner wall are shown in Table 3. In Heaton's analysis, the effects of v on the flow field are underestimated because of linearization; therefore, the Nu numbers obtained by Heaton do not agree very well with the present results. A better agreement is obtained by neglecting v of Eq. (14).

Results and Discussion

Figure 6 shows the Nusselt numbers in the thermal entrance region by considering that the flow field is fully developed and that it is developing. It is obvious that, near the inlet, Nusselt numbers of the developing flow field are larger than those of the fully developed flow field. This is because in the velocity developing region, the boundary layer is thinner; therefore, the drag force is larger, which makes the Nusselt numbers larger. As the HTF flows down from the inlet, the Nusselt numbers of the two different flow fields become closer.

From Eqs. (13) and (14), one can conclude that the Reynolds number will not affect the local heat flow rates. This is effective only when X is defined by $X = x'/RePrD_h$. The effects of changing the initial temperature of the HTF and the PCM and changing the inlet temperature of the HTF of the thermal storage unit on the Nusselt number are shown to be insignificant.

Figure 7 shows the transient temperature distribution of the PCM for flow in the entrance region. The initial temperature of the PCM and HTF is 38°C. The inlet temperature of the HTF is 53°C. Since the temperature of the PCM is initially lower than the melting point temperature, the solid PCM temperature increases to the melting point and melting occurs. However, as time elapses, the solid PCM will approach the melting temperature, a constant temperature. The temperature gradient of the PCM at the inner tube wall will decrease with time. This means that the heat flow rate between the HTF and PCM will decrease with time.

The transient temperature distributions of the HTF are shown in Figs. 8 and 9. Near the inlet, the temperature of the HTF is uniform except at the region near the outer wall of the PCM tube. For the downstream region, the temperature of the HTF at the center portion between r_2 and r_0 is higher than that near the tube wall. This phenomenon is caused by the parabolic velocity distribution. However, as time elapses, the temperature gradient appears to be nonzero only at the region which is near to r_2. From Figs. 8 and 9, one would discover that as X decreases, the temperature gradient at r_2 increases. This characterizes that, near the inlet region, the heat flow

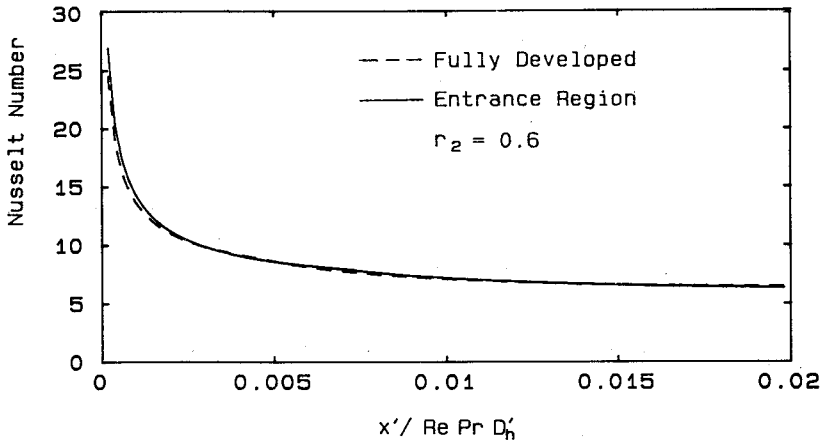

Fig. 6 Effect of developing velocity profiles on Nusselt number.

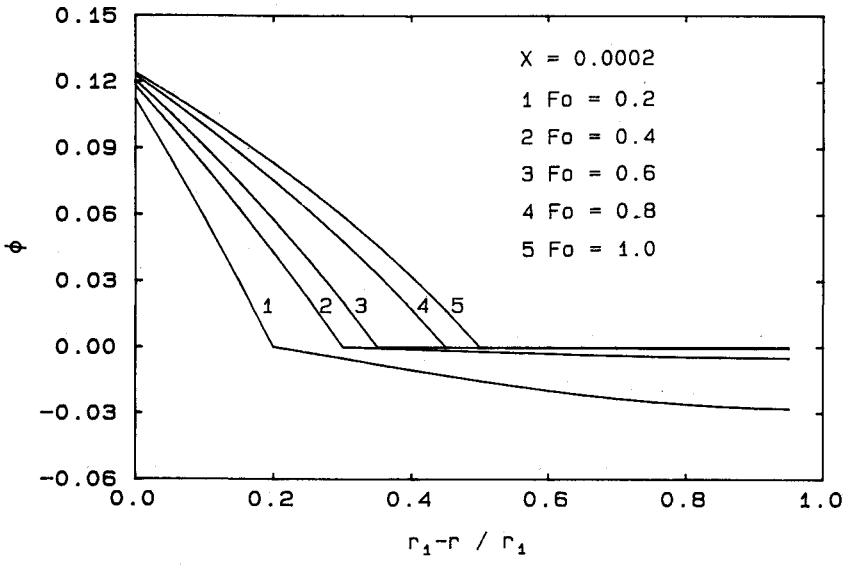

Fig. 7 Temperature distribution of PCM.

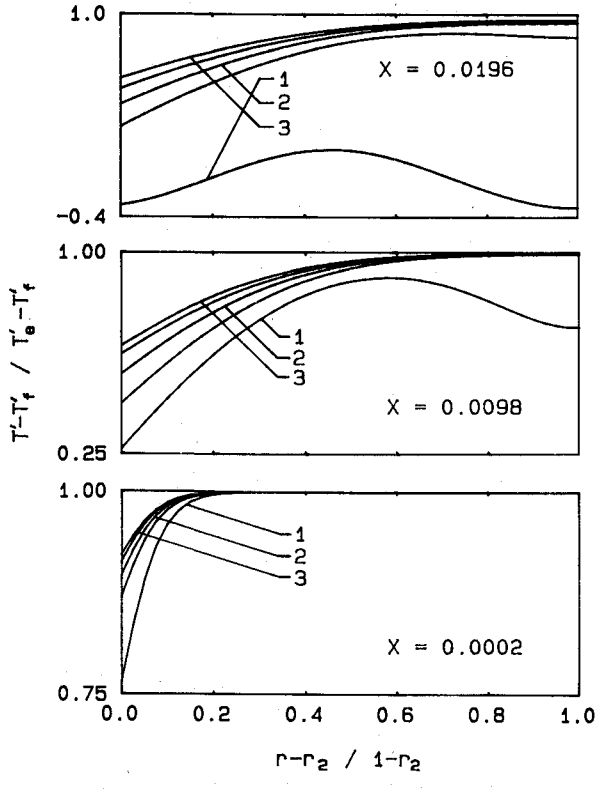

Fig. 8 Temperature distribution of HTF in fully developed region for $r_2 = 0.5$ (curve 1: $Fo = 0.01$; curve 2: $Fo = 0.03$; curve 3: $Fo = 0.05$).

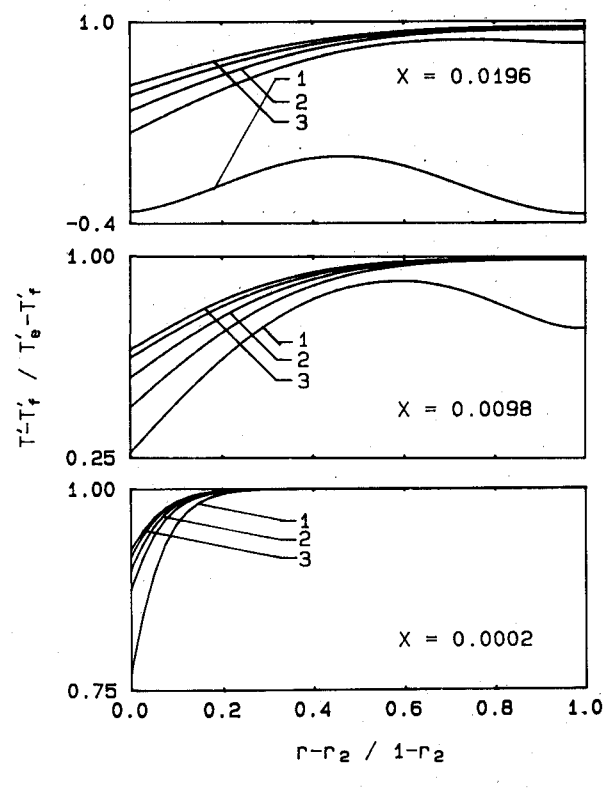

Fig. 9 Temperature distribution of HTF in entrance region for $r_2 = 0.5$ (curve 1: $Fo = 0.01$; curve 2: $Fo = 0.03$; curve 3: $Fo = 0.05$).

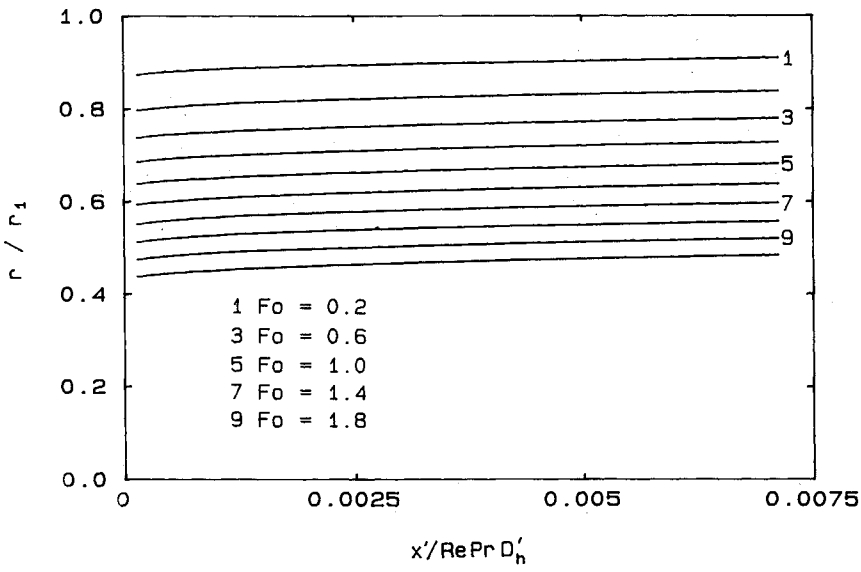

Fig. 10 Time evolution of the solid-liquid interface positions for melting of P116 wax.

rate is larger than that of the downstream region. It is also noted that when time elapses, the local heat flow rates decrease.

For melting of the P116 wax in the latent heat storage unit, both experimental data and predicted results showed fair agreement. However, after the experiment progressed 100 min, air bubbles were generated, which had significant influence on the experimental results, and therefore comparison between the experimental data and predicted results becomes difficult. During the initial melting period, a minimal amount of slumping of the solid PCM was observed. The end plugs of the PCM capsules offered sufficient thermal resistance to allow the solid PCM to remain attached to these plugs for a substantial period of the melting process.

The initial time evolution of the predicted solid/liquid interface positions is plotted on Fig. 10 for constant Reynolds and Prandtl numbers of 683 and 3.93, respectively. It appears clearly on the figure that in the upstream region of the HTF, the melting of the PCM is faster than in the downstream region. This is because in the upstream region the temperature of the HTF is higher and both the temperature and velocity profiles are developing. Figure 10 also indicates that the melting is slower as time increases, which characterizes that the heat flow rates between the HTF and PCM decrease.

Conclusions

Analysis and experiments have been performed for a heat-transfer study of a latent heat storage unit. Melting/freezing problems were solved by a finite-difference method based on the enthalpy formulation. Convection problems of the HTF were solved by first obtaining the velocity distribution and then by solving the energy equation. In addition to the continuity equation and the momentum equation, the integral continuity equation was also used for calculating the velocity distributions.

From the obtained results one can conclude that:

1) The developing temperature profiles increase the Nusselt number significantly. The developing velocity profiles can also increase the Nusselt number. However, the increase is not so significant when compared with the increase caused by the developing temperature profiles.

2) Near the inlet region, the effect of r_2 on the Nusselt number cannot be neglected. The Nusselt number increases with the increase of r_2. In the far downstream region, the effect of r_2 on the Nusselt number is small and can be neglected.

References

[1]Webb, B. W., Moallemi, M. K., and Viskanta, R., "Phenomenology of Melting of Unfixed Phase Change Material in a Horizontal Cylindrical Capsule," American Society of Mechanical Engineers Paper 86-HT-10, 1986.

[2]Bathelt, A. G. and Viskanta, R., "Heat Transfer at the Solid-Liquid Interface During Melting from a Horizontal Cylinder," *International Journal of Heat and Mass Transfer*, Vol. 23, Nov. 1980, pp. 1493–1503.

[3]Ho, C.-J. and Viskanta, R., "Heat Transfer During Inward Melting in a Horizontal Tube," *International Journal of Heat and Mass Transfer*, Vol. 27, May 1984, pp. 705–716.

[4]Pannu, J., Joglekar, G., and Rice, P. A., "Natural Convection Heat Transfer to Cylinders of Phase Change Material Used for Thermal Storage," *AIChE Symposium Series*, Vol. 76, No. 198, 1980, pp. 47–55.

[5]Yao, L. S. and Chen, F. F., "Effects of Natural Convection in the Melted Region Around a Heated Horizontal Cylinder," *Journal of Heat Transfer*, Vol. 102, Nov. 1980, pp. 667–672.

[6]Rieger, H. and Beer, H., "The Melting Process of Ice Inside a Horizontal Cylinder: Effects of Density Anomaly," *Journal of Heat Transfer*, Vol. 108, Feb. 1986, pp. 166–173.

[7]Rieger, H., Projahn, U., and Beer, H., "Analysis of Heat Transport Mechanisms During Melting Around a Horizontal Circular Cylinder," *International Journal of Heat and Mass Transfer*, Vol. 25, Jan. 1982, pp. 137–147.

[8]McCabe, M. E., "Periodic Heat Conduction in Energy Storage Cylinders with Change of Phase," American Society of Mechanical Engineers Paper 86-HT-12, 1986.

[9]Sparrow, E. M. and Hsu, C. F., "Analysis of Two-Dimensional Freezing on the Outside of a Coolant-Carrying Tube," *International Journal of Heat and Mass Transfer*, Vol. 24, Aug. 1981, pp. 1345–1357.

[10]Shamsundar, N., "Formulae for Freezing Outside a Circular Tube with Axial Variation of Coolant Temperature," *International Journal of Heat and Mass Transfer*, Vol. 25, Oct. 1982, pp. 1614–1616.

[11]Asgarpour, S. and Bayazitoglu, Y., "Heat Transfer in Laminar Flow with a Phase Change Boundary," *Journal of Heat Transfer*, Vol. 104, Nov. 1982, pp. 678–682.

[12]Reynolds, W. C., Lundberg, R. E., and McCuen, P. A., "Heat Transfer in Annular Passages. General Formulation of the Problem for Arbitrarily Prescribed Wall Temperatures or Heat Fluxes," *International Journal of Heat and Mass Transfer*, Vol. 6, June 1963, pp. 483–493.

[13]Lundberg, R. E., McCuen, P. A., and Reynolds, W. C., "Heat Transfer in Annular Passages. Hydrodynamically Developed Laminar Flow with Arbitrarily Prescribed Wall Temperatures or Heat Fluxes," *International Journal of Heat and Mass Transfer*, Vol. 6, June 1963, pp. 495–529.

[14]Worsoe-Schmidt, P. M., "Heat Transfer in the Thermal Entrance Region of Circular Tubes and Annular Passages with Fully Developed Laminar Flow," *International Journal of Heat and Mass Transfer*, Vol. 10, April 1967, pp. 541–551.

[15]Hatton, A. P. and Quarmby, A., "Heat Transfer in the Thermal Entry Length with Laminar Flow in an Annulus," *International Journal of Heat and Mass Transfer*, Vol. 5, Oct. 1962, pp. 973–980.

[16]Sutherland, W. A. and Kays, W. M., "Heat Transfer in an Annulus with Variable Circumferential Heat Flux," *International Journal of Heat and Mass Transfer*, Vol. 7, Nov. 1964, pp. 1187–1194.

[17]Murakawa, K., "Heat Transfer in Entry Length of Double Pipes," *International Journal of Heat and Mass Transfer*, Vol. 2, No. 3, 1961, pp. 240–251.

[18]Liron, N. and Gillis, J., "Stokes Flow in an Annular Region," *Journal of Applied Mechanics*, March 1970, pp. 29–33.

[19]Heaton, H. S., Reynolds, W. C., and Kays, W. M., "Heat Transfer in Annular Passages. Simultaneous Development of Velocity and Temperature Fields in Laminar Flow," *International Journal of Heat and Mass Transfer*, Vol. 7, July 1964, pp. 763–781.

[20]Lamb, H., *Hydrodynamics*, 5th ed., Cambridge University Press, London, 1924.

[21]O'Dell, M. P., Sheffield, J. W., and Wen, C., "An Analytical and Experimental Examination of a Latent Thermal Management System," AIAA Paper 87-1490, 1987.

[22]Viskanta, R. and Gau, C., "Inward Solidification of a Superheated Liquid in a Cooled Horizontal Tube," *Warme-und Stoffubertragung*, Vol. 17, No. 1, 1982, pp. 39–46.